



# Numerical Solution of Stagnation Point Flow of Non-Newtonian Fluid and Heat Transfer over a Porous Medium under Effect of Thermal Radiation and Magnetic Field

Hamsa D. Saleem<sup>1,\*</sup>, Iman H. Al-Obaidi<sup>1</sup>, Alaa A. Hammodat<sup>1</sup>

<sup>1</sup> *Department of Mathematics, College of Education for Pure Sciences, University of Mosul, Mosul, 41001, Iraq*

---

**Abstract.** We study three key topics in this article, including Casson fluid flow at its stagnation point, heat transfer in the current magnetic field, and thermal radiation. Several equations related to coupled mass, momentum, and energy are controlled by the mathematical model. This is accomplished by using appropriate transformations to study dimensionless partial differential equations of motion, energy, and continuity. The Adam-Bashforth method is used to solve several nonlinear dimensionless partial differential equations. The analysis is based both on analytic and numerical representations of the impact of parameters which are relevant to the analysis, such as the Casson parameter  $\beta$ , porosity parameter  $K$ , magnetic field  $\mathcal{M}$ , mixed convection parameter  $\gamma$ , and thermal radiation  $\mathcal{R}$ . Finally, using the Adam-Bashforth approach, we are able to determine velocity profiles as well as temperature profiles.

**2020 Mathematics Subject Classifications:** 65Lxx, 65Mxx, 80Mxx

**Key Words and Phrases:** Stagnation point flow, Heat transfer, Shrinking/stretching sheet, Skin Friction coefficient, Local Nusselt

---

## 1. Introduction

Stagnation point flow, which can happen in the presence of both stationary and moving bodies in a fluid, is the term for the fluid motion that occurs immediately adjacent to the stagnation section of a compact surface. With the calculation of skin friction and heat/mass transfer close to stagnation regions of bodies in high-speed movements, the proposal of thrust airs and circular diffusers, effort discount, transpiration cooling, and thermal oil retrieval, among other physical effects, more emphasis is placed on the flow at a stagnation point. The two-dimensional flow of a fluid close to a stagnation point was

---

\*Corresponding author.

DOI: <https://doi.org/10.29020/nybg.ejpam.v16i3.4786>

*Email addresses:* [alaahammodat@uomosul.edu.iq](mailto:alaahammodat@uomosul.edu.iq) (A. A. Hammodat),

[hamsa\\_dawood@uomosul.edu.iq](mailto:hamsa_dawood@uomosul.edu.iq) (H. D. Saleem), [emanhashem1986@uomosul.edu.iq](mailto:emanhashem1986@uomosul.edu.iq) (I. H. Al-Obaidi)

first described by Hiemenz [7] and is now a well-known fluid dynamics problem. Several researchers have made contributions to this field. Ghosh et al., recently researched the effects of Hall on MHD flow in a revolving formation with effortlessly showing walls in 2009. The discovery has instantaneous application in MHD energy creators, but according to the authors' facts, it has not yet been discussed in the literature on engineering sciences [4]. In 2010 [19], Tasawar H. and Meraj M. conducted research on the impact of recent radioactivity on the turbulent, varied convection flow of a Jeffrey liquid beyond a permeable, plumb-extending surface. In 2011, Norfifah B. and Anuer I. carried out an arithmetical examination of a stagnation-point flow approaching a sheet that was non-linearly expanding or contracting while submerged in a viscous fluid. The outward flow velocity attacks usually the stretching or shrinking slip, and the stretching or shrinking velocity is presumptive of the form  $U_x$ , where  $x$  is the reserve after the stagnation point, and  $m$  is a persistent wave [13].

In 2013, Karthikeyan et al., [10] analyzed how heat radiation affected the issue of instable magneto-convection flow of an electrically directing fluid past a semi-unlimited perpendicular spongy platter inundated in a porous average with time-reliant suction. In 2014, Rajesh S. and Anuar I. conducted a numerical study to examine the boundary sheet flow of a Cu-water-built nanofluid with heat transfer concluded by a stretching sheet. In contrast to no slip at the boundary, the second-order velocity slip flow model is preferred [14]. The same year, Hayat et al., [6] explored the stagnation-point stream of second-grade fluid with an asymmetrical stretching exterior in the presence of a fluctuating free stream.

Veeresh et al., examined the heat and mass transfer properties of a viscous, incompressible, free convective, chemically mercurial, radiative, and electrically conducting fluid flowing on an affectingly frenetic porous plate in 2015 [21]. This was done through the occurrence of a temperature-independent heating basis and joule heating. According to the assumptions that the upper and lower channels, respectively, are porous and non-porous, Joseph et al., investigated the instable MHD free convective flow of two immiscible liquids in a straight network with heat and mass transfer in the same year [9]. Awaludin I. et al., demonstrated a stable stagnation point flow of a viscous fluid in the direction of that linearly stretching or shrinking sheet of constant temperature in 2016 [8]. Mahantesh, M., and Shilpa, J. investigated the Casson fluid's stagnation point flow and heat transfer analyses over a stretching and contracting sheet in a porous medium that same year [12]. Siti K. et al., research on unstable magnetohydrodynamic (MHD) stagnation point flow across a stretching or contracting sheet in a viscous fluid with viscous dissipation and ohmic heating was published in 2017 [17]. At the same year, Raju et al., investigated the effect of thermal diffusion on an unsteady magnetohydrodynamic free convection, heat and mass transfer, electrically conducting non-Newtonian Casson fluid flow over on a vertically inclined surface taken in to the account with constant heat flux [15].

In 2018 [1], Babu S. et al., used numerical analysis to examine how magnetic fields and radiation affect heat and mass transfer over a stretched sheet embedded in a porous medium containing viscous micropolar fluid. The explanation of the fixed two-dimensional

MHD stagnation point flow of non-Newtonian fluid and heat transfer of a stretching and astringent sheet in the incidence of thermal radiation was published in 2019 [5] by Hammodat A. and Basheer A. The three-dimensional incompressible viscoelastic fluid flow through a porous stretching and contracting sheet with hybrid copper and alumina nanoparticles (Cu Al<sub>2</sub>O<sub>3</sub>) in base fluid water  $H_2O$  was studied by Ulavathi S. and et al. in 2022 [20]. At the same year, Mebarek-Oudina F. and Chabani I. studied the magnetic fields, porous media, and Nano-fluids in different heat transfer applications is discussed mainly in the solar thermal field [11]. Also, at 2022, Sunthrayuth et al., described the exact solutions of fractional Casson fluid through a channel under the effect of MHD and porous medium. The unsteady fluid motion of the bottom plate, which is confined by parallel but perpendicular sidewalls, supports the flow [18]. In 2023, Shafique et al., examined the effect of incompressible Jeffrey fluid flow over an infinite vertical plate with slip and sorret effects. The MHD flow together with heat and mass transfer is considered. Initially, the dimensional equations have been made nondimensional and then solved these equations via Laplace transform [16]. The steady two-dimensional MHD stagnation point flow of a Casson fluid as well as the heat transfer of a stretching or contracting sheet in the presence of thermal radiation are both investigated in the current study. The regulatory partial differential equations must undergo the necessary likeness adjustments in order to be transformed into non-linear ordinary differential equations. These ordinary differential equations are numerically resolved using the Adam-Bashforth (AB) method. Several graphics that show how physical factors affect flow and heat transmission are presented along with the numerical results.

Table 1: Nomenclature

$u, v$	Velocity Components ( $ms^{-1}$ )
$\sigma^*$	Stefan-Boltzmann
$x, y$	Cartesian Coordinates ( $m$ )
$u_e(x)$	external flow velocity
$\nu$	Kinematic fluid viscosity ( $m^2s^{-1}$ )
$K_1$	Absorption coefficient
$\rho$	Fluid density ( $Kgs^{-1}$ )
$\alpha$	Thermal diffusivity ( $m^2s^{-1}$ )
$\beta$	Casson parameter
$K^*$	Porosity parameter
$K$	permeability of the porous medium ( $Hm^{-1}$ )
$\gamma$	Mixed convection parameter
$\sigma$	Electrical conductivity of the fluid ( $ohmm)^{-1}$
$\mathcal{R}$	Thermal radiation parameter
$B^*$	Strength of magnetic field applied in the $y$ direction ( $Am^{-1}$ )
$\mathcal{M}$	Magnetic component
$T$	Temperature
$\mathcal{C}_f$	Skin friction coefficient ( $Nm^{-2}$ )
$c_p$	Specific heat with constant pressure ( $JK^{-1}Kg^{-1}$ )
$\mathcal{N}_u$	Local Nusselt number
$q_r$	Radiative heat flux ( $W$ )
$g$	Acceleration ( $ms^{-2}$ )
$\Psi$	Stream function.
$\tau_0$	Shear Stress ( $Nm^{-2}$ )
$q_0$	Heat Flux from the Sheet
$R_e$	Local Reynolds Number
$T_\infty$	The Surface Temperature ( $K$ )
$u_\infty(x)$	The Velocity of Stretching/Shrinking Sheet
$b$	The Stretching Rate
$0$	The Stagnation Point

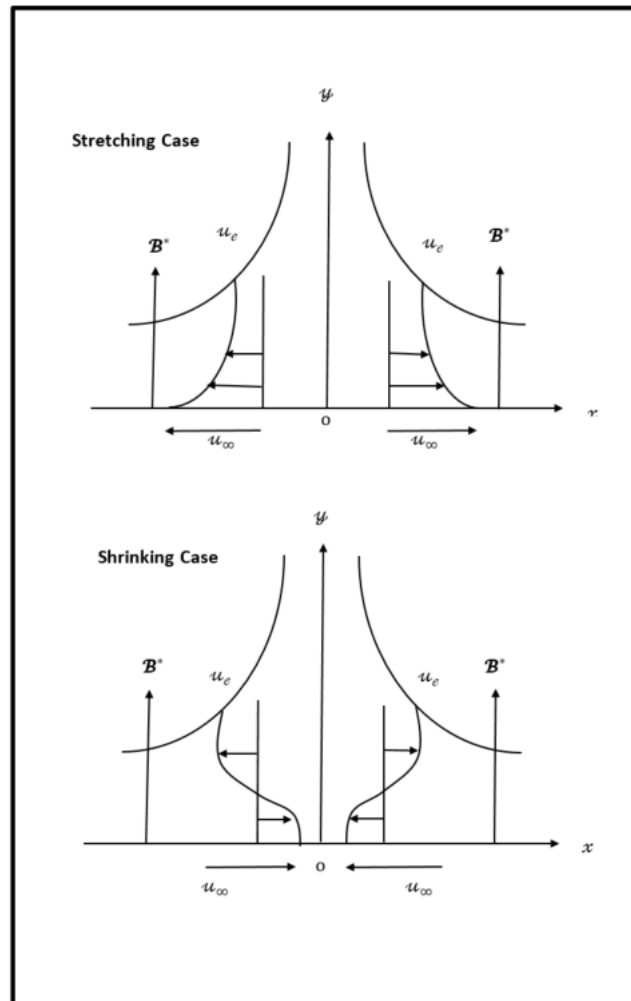


Figure 1: Physical geometry.

## 2. Formulation of Problems and Mathematical Models:

Consider an incompressible stream of electrically conducting Casson fluid at a fixed stagnation point that is produced by stretching and shrinking a sheet in a porous medium. The stretching or shrinking sheet's  $x$ -axis is measured along it, and the  $y$ -axis is restrained normal to it, when calculating the cartesian co-ordinates  $x$  and  $y$  with the origin  $0$  at the stagnation point. The outward temperature  $T_\infty$  is fixed, and it is assumed that the external flow velocity is given by the expression  $u_e(x) = ax$ , where  $a > 0$  is the strength of the stagnation flow. Furthermore, it is presumable that the stretching or shrinking sheet's velocity is given by the equation  $u_\infty(x) = bx$ , where  $b$  is the stretching rate with  $b > 0$  and  $b < 0$  are for the stretching or shrinking case correspondingly. For the flow in the porous

medium, the boundary layer equations can be expressed as:

$$\frac{\partial u}{\partial x} + \frac{\partial v}{\partial y} = 0, \tag{1}$$

$$u \frac{\partial u}{\partial x} + v \frac{\partial u}{\partial y} = u_e \frac{\partial u_e}{\partial x} + \nu \left(1 + \frac{1}{\beta}\right) \frac{\partial^2 u}{\partial y^2} + \left(1 + \frac{1}{\beta}\right) \frac{\nu}{K} (u_e - u) + g\beta(T - T_0) - \frac{\sigma \mathcal{B}^{*2}}{\rho} u, \tag{2}$$

$$u \frac{\partial T}{\partial x} + v \frac{\partial T}{\partial y} = \alpha \frac{\partial^2 T}{\partial y^2} - \frac{1}{\rho C_p} \frac{\partial q_r}{\partial y}. \tag{3}$$

Using the Roseland approximation for radiation [3].

$$q_r = - \left(\frac{4\sigma^*}{3K_1}\right) \frac{\partial T^4}{\partial y}, \tag{4}$$

is obtained. According to our hypothesis, the expansion of  $T^4$  into Taylor's series is permitted by the temperature change within the flow. Escalating  $T^4$  about  $T_0$  and ignoring advanced-order reports we get  $T^4 = 4T_0^3 T - 3T_0^4$  [2]. Equation (3) becomes:

$$u \frac{\partial T}{\partial x} + v \frac{\partial T}{\partial y} = \left(\alpha + \frac{16\sigma T_0^3}{3\rho C_p K_1}\right) \frac{\partial^2 T}{\partial y^2}. \tag{5}$$

Depending on the encircling restrictions:

$$\left. \begin{aligned} u_\infty(x) &= bx, & T &= T_\infty, & \text{at } y &= 0, \\ u_e(x) &= ax, & T &= T_0, & \text{at } y &\rightarrow \infty, \end{aligned} \right\}. \tag{6}$$

For equations (2) and (5) of the ordinary differential type, we present the resulting comparison variables.

$$\tau = \left(\frac{u_e(x)x}{\nu}\right)^{1/2} \frac{y}{x}, \quad \Psi = (\nu x u_e)^{1/2} F(\tau), \quad \vartheta(\tau) = \frac{T - T_0}{T_\infty - T_0}. \tag{7}$$

The function of streams  $\Psi$ , described as:  $u = \frac{\partial \Psi}{\partial y}$  and  $v = -\frac{\partial \Psi}{\partial x}$ , which satisfies equation (1), and equations (2), (5), and (6) lead to the following conclusion:

$$\left(1 + \frac{1}{\beta}\right) (F''' + K(1 - F')) + FF'' - F'^2 - \mathcal{M}F' + \gamma\vartheta + 1 = 0, \tag{8}$$

$$\vartheta'' + \mathcal{R}F\vartheta' = 0. \tag{9}$$

Similarly, the boundary conditions (6) reduces to:

$$\left. \begin{aligned} F(\tau) &= 0, & F'(\tau) &= \frac{b}{a} = c, & \vartheta(\tau) &= 0 & \text{at } \tau &= 0, \\ F'(\tau) &\rightarrow 1, & \vartheta(\tau) &\rightarrow 0, & & & \text{at } \tau &\rightarrow \infty, \end{aligned} \right\}. \tag{10}$$

Skin friction factor  $\mathcal{C}_f$  and average Nusselt ratio  $\mathcal{N}_u$  are defined as:

$$\mathcal{N}_u = \frac{xq_0}{K(T_\infty - T_0)}, \quad \text{and } \mathcal{C}_f = \frac{\tau_0}{\rho u_e^2(x)}, \tag{11}$$

where  $\tau_0$  which is greater along the stretching sheet: skin resistance or shear stress and  $q_0$  is the heat flux from the sheet defined as:

$$\tau_0 = \mu \left( \frac{\partial u}{\partial y} \right)_{y=0}, \quad \text{and } q_0 = -K \left( \frac{\partial T}{\partial y} \right)_{y=0} \tag{12}$$

Thus, we get the skin friction factor  $\mathcal{C}_f$  and the local Nusselt ratio  $\mathcal{N}_u$  as follows:

$$\mathcal{C}_f(R_e)^{1/2} = F''(0), \quad \text{and } \mathcal{N}_u(R_e)^{-1/2} = -\vartheta'(0), \tag{13}$$

where  $R_e = \frac{xu_e(x)}{\nu}$  is the local Reynolds number.

### 3. Approach to a Solution:

In this study, we propose and investigate an explicit linear multistep methods scheme called the AB formula which is one of the well-known predictor multistep methods. The explicit and implicit types of AB are the two types that exist. The implicit kind is identified as the Adams-Moulton (AM) method, and the name Moulton became associated with it because he realized it could be used in conjunction with the AB method as a predictor, corrector, or approach. John Couch Adams developed the AB method, also known as the explicit type, in 1883. These methods possess relatively good stability and convergence properties. The Adams technique is based on the idea of approximating the integrand with a polynomial of interval using a  $k$ th order polynomial, resulting in a  $k + 1$  order procedure where, at each step, we solve the equations (8) and (9) pertaining to the boundary equation (10) by providing a set of starting values [18].

### 4. Results and Discussions:

Many dimensionless parameter values, including Casson parameters  $\beta$ , porosity parameters  $K$ , magnetic field parameters  $\mathcal{M}$ , mixed convection parameters  $\gamma$ , and thermal radiation  $\mathcal{R}$ , are computed numerically in order to evaluate the physical importance of the relevant problem. The computed result is displayed together with the velocity and temperature shapes, and the physical rationale is provided below. Following are the temperature and velocity distributions:

#### 4.1. The Casson parameters impact $\beta$ :

Figures 2 and 3 show how the flow field's velocity and temperature profiles change when the Casson parameters  $\beta$  are varied while keeping all other variables constant. The

flow field's velocity decreases with decreasing Casson values, as seen in Figure 3. Figure 4 demonstrates that the effect of raising Casson values  $\beta$  on temperatures is minimal.

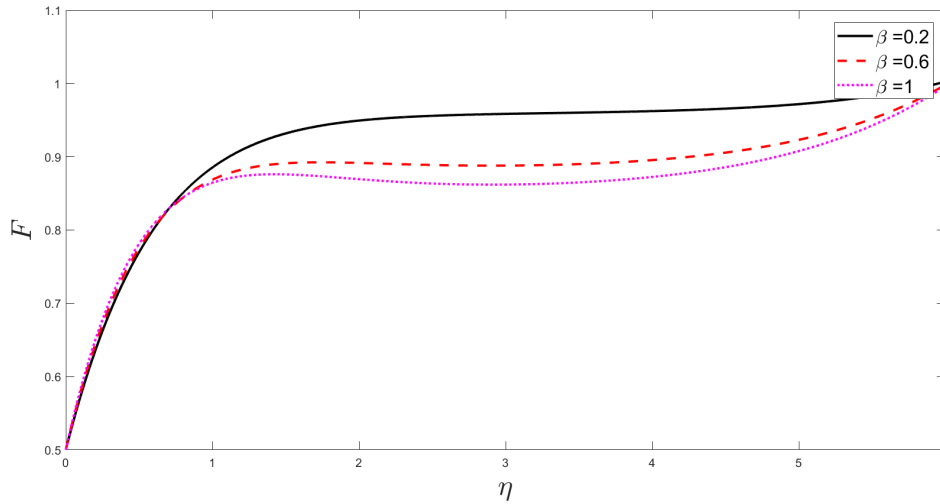


Figure 2: Variation of velocity profile when  $\beta=0.2,0.6,1$ .

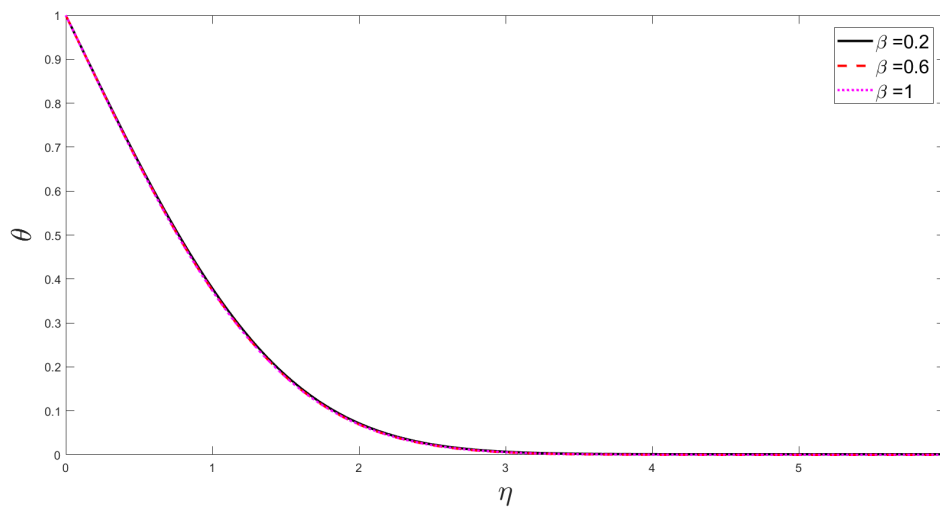


Figure 3: Temperature profile variation for different values of  $\beta=0.2,0.6,1$ .

#### 4.2. Effect of porosity parameter K:

Analog to Figure 4, Figure 5 illustrates the effects of the coefficient values K on the temperature and velocity profiles if the other parameters stay unchanged. The velocity



profile is enhanced at higher values of  $K$ , as shown in Figure 4. But in Figure 5, the effect of raising the porosity parameter  $K$  is minimal for temperatures.

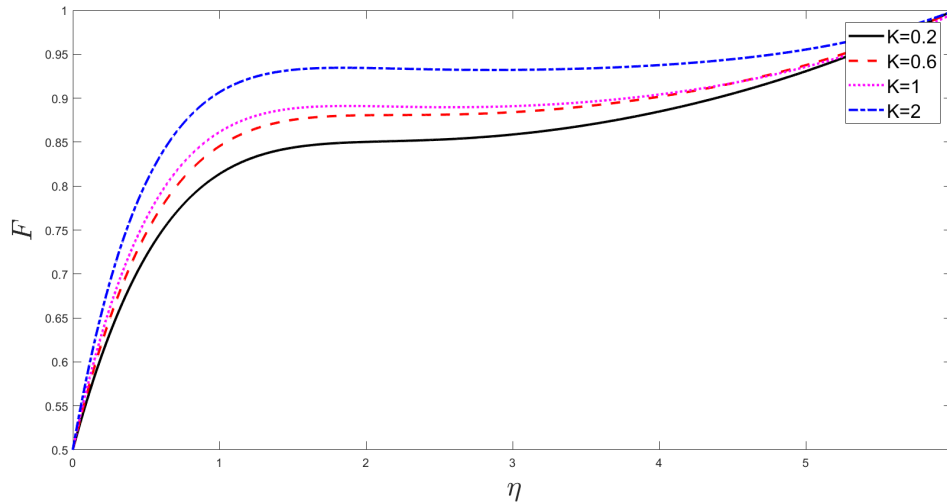


Figure 4: Change of Velocity Distribution for Distinct  $K=0.2,0.6,1,2$ .

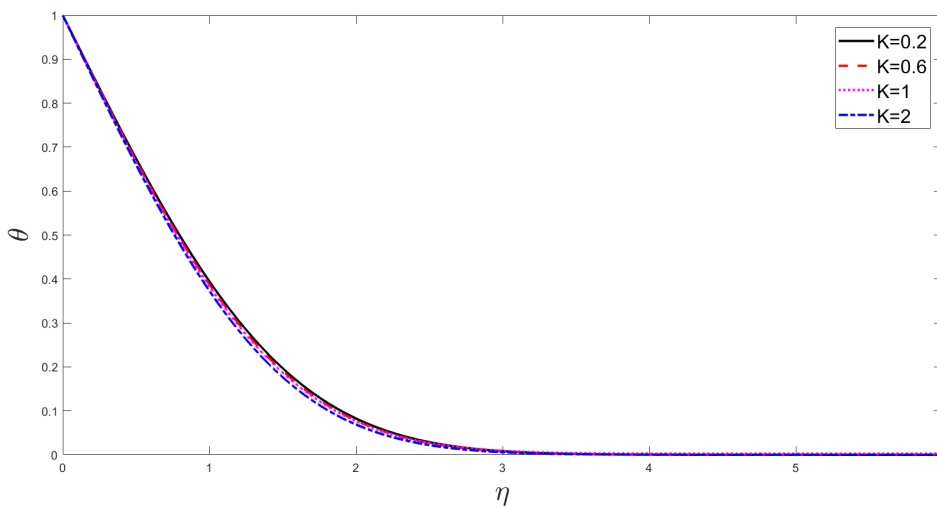


Figure 5: Temperature and Concentration Variance for Distinct Values of  $K=0.2,0.6,1,2$ .

### 4.3. Effect of mixed convection parameter $\gamma$ :

The flow field's velocity decreases as the mixed convection parameter's value  $\gamma$  rises as shown in Figure 6. The flow field's velocity decreases. Figure 7 indicates that temperature profiles are rising due to lower values  $\gamma$ .

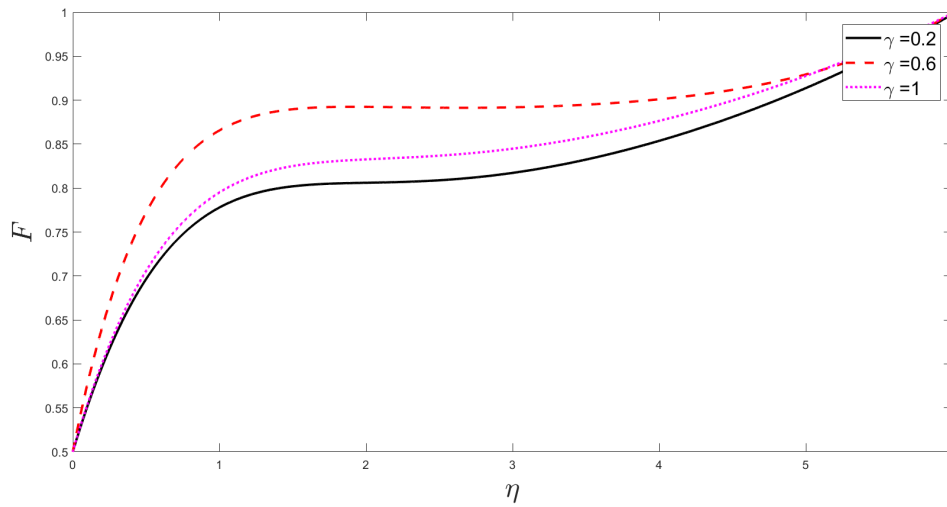


Figure 6: Distinction of Speed Shape for Several Values of  $\gamma=0.2,0.6,1$ .

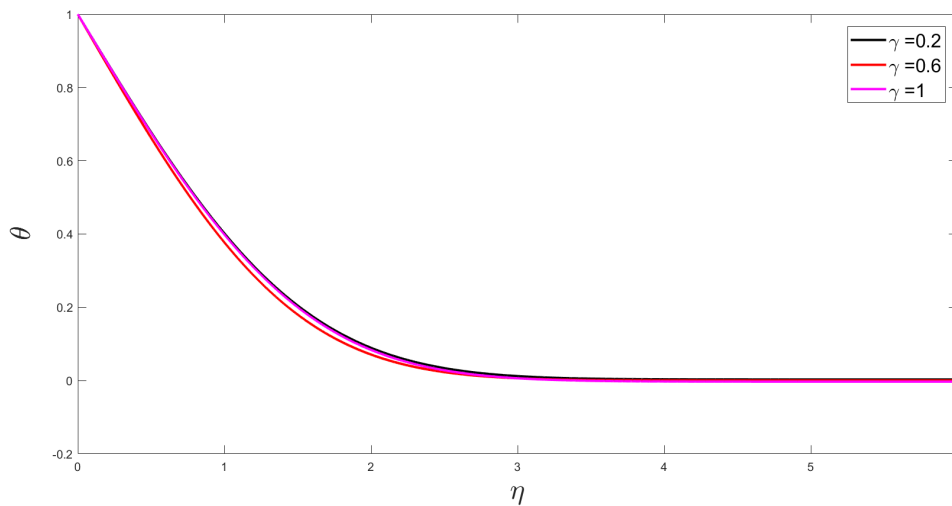


Figure 7: Local Temperature Variance for Different Values of  $\gamma = 0.2, 0.6, 1$ .

#### 4.4. $\mathcal{M}$ 's Magnetic Field's Impact:

Figures 8 and 9 show how the flow field's velocity and temperature profiles change when the magnetic parameter  $\mathcal{M}$  is varied while other parameters remain constant. The flow field's velocity decreases with decreasing magnetic field values  $\mathcal{M}$ , as seen in Figure 8. Figure 9 shows that the rising values of magnetic field  $\mathcal{M}$  cause temperature profiles to rise.

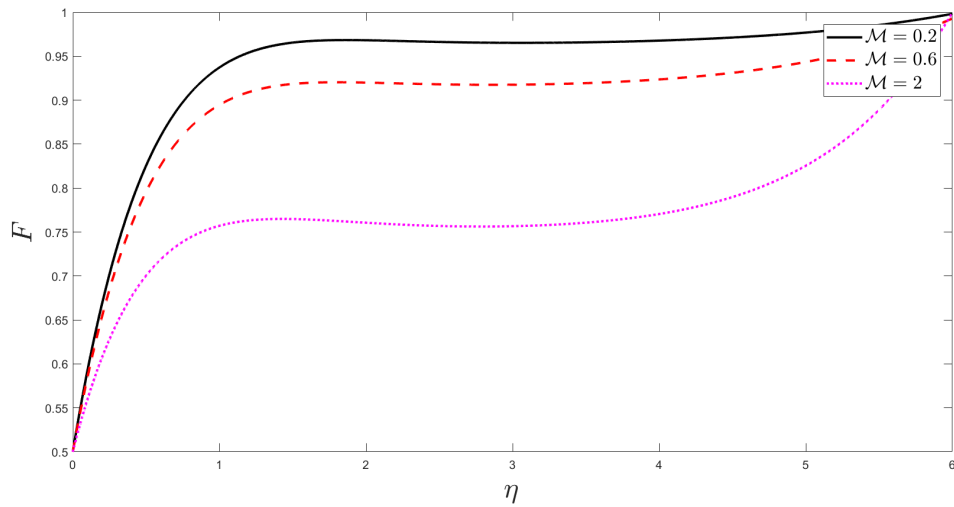


Figure 8: Change in the Velocity Profile at Different Values of  $\mathcal{M} = 0.2, 0.6, 2$ .

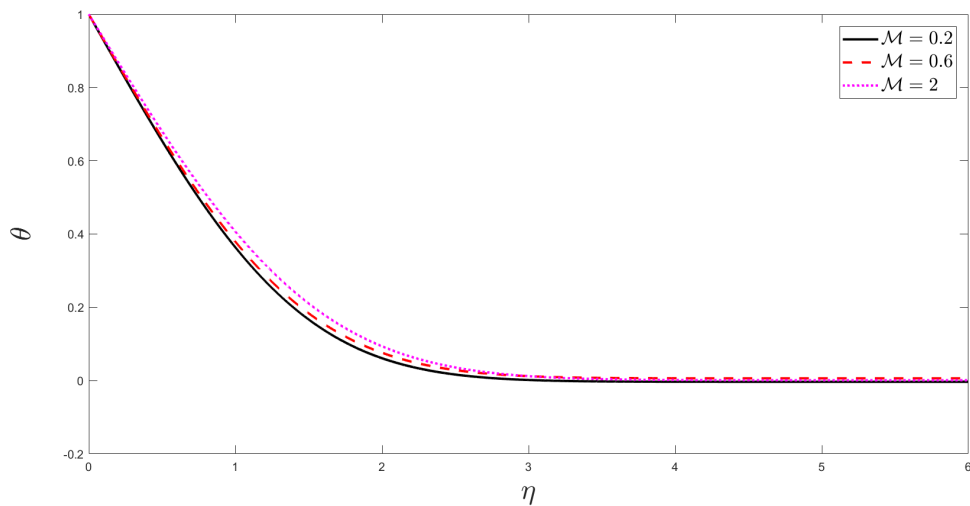


Figure 9: Profile of Temperature Variation for  $\mathcal{M} = 0.2, 0.6, 2$ .

#### 4.5. Effect of Radiation Parameter $\mathcal{R}$ :

Figures 10, 11 demonstrate how the temperature and velocity profiles both rise when the radiation parameter  $\mathcal{R}$  falls.

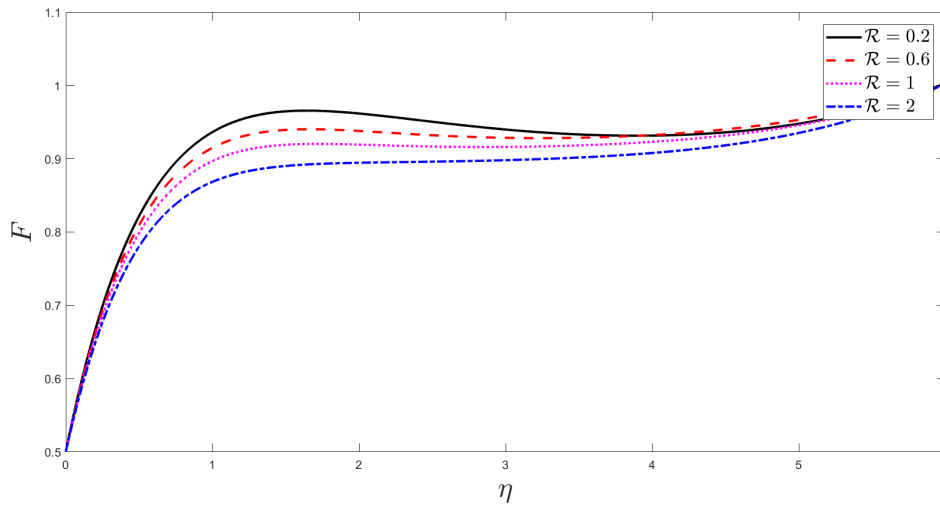


Figure 10: Modify of Velocity Profile for Variable  $\mathcal{R} = 0.2, 0.6, 1, 2$  Values.

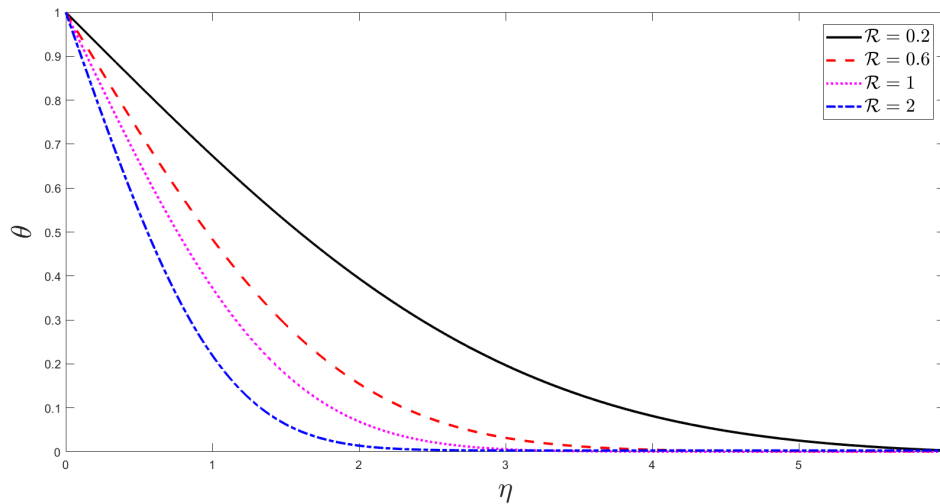


Figure 11: Temperature Profile Variation for Varied Values of  $\mathcal{R} = 0.2, 0.6, 1, 2$ .

### 5. Conclusion

The thermal radiation impact is taken into account as the MHD stagnation point flow of Casson fluid and heat transfer over a stretching or shrinking sheet are explored. The governing equations are converted to self-similar ordinary differential equations (ODEs) via the similarity transformation, and the AB method is then used to solve them. The study's findings can be summed up as follows:

1. The velocity is increase when the Casson parameter  $\beta$  is decrease.
- 2 .With higher Magnetic values  $\mathcal{M}$  and Radiation parameter  $\mathcal{R}$  , the velocity distribution slows down.
3. The velocity of fluid is increase when the porosity parameter  $K$  is increase.
4. The velocity distribution is increase when the mixed convection parameter  $\gamma$  is increase.
- 5.The Temperature of fluid decays down for larger values of magnetic field  $\mathcal{M}$ . As well as, The temperatures of fluid increase for small values of the Radiation  $\mathcal{R}$  and the mixed convection parameter  $\gamma$  . While the effect of Casson coefficient  $\beta$  and Hartmann number  $\mathcal{M}$  is slight on temperature of fluid.

### Acknowledgements

The College of Education for Pure Science at University of Mosul was helpful in enhancing the project's quality, and the writers gratefully acknowledge their cooperation.

### References

- [1] S. Babu, S. Venkateswarlu, and K. Jaya. Effect of magnetic field and radiation on mhd heat and mass transfer of micropolar fluid over stretching sheet with sores and dufour effects. 13(12):10991–11000, 2018.
- [2] K. Bhattacharyya. Mhd stagnation- point flow of casson fluid and heat transfer over a stretching sheet with thermal radiation. *Journal of Thermodynamics*, 2013(Article ID 169974), 2013.
- [3] M.Q. Brewster. Thermal radiative transfer properties. *John Wiley and Sons*, 1972.
- [4] S. Ghosh, O. Anwar Beg, and M. Narahari. Hall effects on mhd flow in a rotating system with heat transfer characteristics. *Meccanica*, (44):741—765, 2009.
- [5] A. Hammodat and A. Basheer. Mhd stagnation-point flow of non-newtonian fluid and heat transfer over stretching/shrinking sheet in a porous medium. *J. Edu. Sci.*, 28(1), 2019.
- [6] T. Hayat, M. Qasim, S. Shehzad, and A. Alsaedi. Unsteady stagnation point flow of second grade fluid with variable free stream. *Alexandria Engineering Journal*, 53(2):455–461, 2014.
- [7] F. Homann. Der einfluss grosser z higkeit bei der str mung um den zylinder und um die kugel. *Z Angew Math Mech*, (16):153–64, 1936.

- [8] I.Awaludin, P. Weidman, and A. Ishak. Stability analysis of stagnation-point flow over a stretching/shrinking sheet. *AIP Advances*, 6(4), 2016.
- [9] K. Joseph, A. Peter, P. Asie, and S. Usman. The unsteady mhd free convective two immiscible fluid flows in a horizontal channel with heat and mass transfer. *INTERNATIONAL JOURNAL OF MATHEMATICS AND COMPUTER RESEARCH*, 30(5):954–972, 2015.
- [10] S. Karthikeyan, M. Bhuvanewari, S. Rajan, and S. Sivanandam. Thermal radiation effects on mhd convective flow over a plate in a porous medium by perturbation technique. *App. Math. and Comp. Intel.*, 2(1):75–83, 2013.
- [11] F. Mebarek-Oudina and I. Chabani. Review on nano-fluids applications and heat transfer enhancement techniques in different enclosures. *Journal of Nanofluids.*, 11:155–168, 2022.
- [12] M.Mahantesh and J. Shilpa. Stagnation point flow of non –newtonian fluid and heat transfer over a stretching /shrinking sheet in a porous medium. *Chemical and process engineering research*, 46, 2016.
- [13] B. Norfifah and I. Anuer. Similarity solutions for the stagnation-point flow and heat transfer over a nonlinearly stretching/shrinking sheet. *Sains Malaysiana*, 11(40):1297–1300, 2011.
- [14] S. Rajesh and I. Anuar. Second order slip flow of cu-water nanofluid over a stretching sheet with heat transfer. *WSEAS TRANSACTIONS on FLUID MECHANICS*, 9:26–33, 2014.
- [15] R. Raju, B. Mahesh, and G. Raddy. Influence of angle of inclination on unsteady mhd casson fluid flow past a vertical surface filled by porous medium in presence of constant heat flux chemical reaction and viscous dissipation. *journal of nanofluids. Journal of Nanofluids.*, 6:668–679, 2017.
- [16] A. Shafique, M. Ramzan, Z. Ikram, M. Amir, and M. Nazar. Mhd flow of jeffrey fluid with heat absorption and thermo-diffusion. *Frontiers in Heat and Mass Transfer (FHMT).*, 20(4):1–10, 2023.
- [17] K. Siti, A. Ishak, and I. Pop. Unsteady mhd flow and heat transfer over a shrinking sheet with ohmic heating. *Chinese Journal of Physics*, 55(4):1626–1636, 2017.
- [18] P. Sunthrayuth, A. Alderremy, F. Ghani, A. Tchalla, Sh. Aly, and Y. Elmasry. Unsteady mhd flow for fractional casson channel fluid in a porous medium: An application of the caputo-fabrizio time-fractional derivative. *Journal of Function Spaces.*, 11, 2022.
- [19] H. Tasawar and M. Meraj. Influence of thermal radiation on the unsteady mixed convection flow of a jeffrey fluid over a stretching sheet. *Z. Naturforsch.*, (65):711–719, 2010.

- [20] S. Ulavathi, A. Thippesswamy, L. David, S. Najla, and SH. Mohsen. An mhd flow of non-newtonian fluid due to a porous stretching/shrinking sheet with mass transfer. *Sustainability*, 14(12), 2022.
- [21] C. Veeresh, S. Vijayakumar, and D. Praveena. Heat and mass transfer in mhd free convection chemically reaction and radiative flow in a moving inclined porous plate with temperature dependent heat source and joul heating. *Best: International Journal of Management, Information Technology and Engineering (BEST: IJMITE)*, 3(11):63–74, 2015.